

LETTERS

The deterministic nature of earthquake rupture

Erik L. Olson¹ & Richard M. Allen²

Understanding the earthquake rupture process is central to our understanding of fault systems and earthquake hazards. Multiple hypotheses concerning the nature of fault rupture have been proposed but no unifying theory has emerged^{1–12}. The conceptual hypothesis most commonly cited is the cascade model for fault rupture^{1,3,10,13}. In the cascade model, slip initiates on a small fault patch and continues to rupture further across a fault plane as long as the conditions are favourable. Two fundamental implications of this domino-like theory are that small earthquakes begin in the same manner as large earthquakes and that the rupture process is not deterministic—that is, the size of the earthquake cannot be determined until the cessation of rupture. Here we show that the frequency content of radiated seismic energy within the first few seconds of rupture scales with the final magnitude of the event. We infer that the magnitude of an earthquake can therefore be estimated before the rupture is complete. This finding implies that the rupture process is to some degree deterministic and has implications for the physics of the rupture process.

In the cascade model, faults are divided into patches of varying size and shape. When an earthquake initiates on one patch, slip on that patch can lead to slip on the adjacent patches if the rupture energy and the state of stress on these adjacent patches are favourable. An earthquake continues spreading from patch to patch until there is insufficient energy to rupture the next patch, at which point the rupture stops. This model is consistent with the concepts of seismic moment and magnitude. Moment is physically related to both rupture area, A , and average slip, \bar{D} , by the relation $M_o = \mu A \bar{D}$ where M_o is the seismic moment and μ is the shear modulus. Moment magnitude, M_w , scales with the seismic moment and is therefore similarly related to A and \bar{D} (ref. 14). Given this framework, it is not possible to know the magnitude of an earthquake until the rupture has stopped.

Throughout the last decade, the seismological community has debated whether the first few seconds of the P wave (the first few seconds of radiated energy) provides information about the final magnitude of an earthquake before the rupture is complete^{3,9–11}. Much of the debate has focused on the time-domain characteristics of the P wave. However, evidence for a scaling relation between the frequency content of the first few seconds of the P wave and the final magnitude has also emerged^{15–18}. Using an approach similar to Nakamura¹⁵, Allen and Kanamori¹⁶ measured the predominant period, τ_p , from the first 4 s of the P-wave arrival at multiple seismic stations in southern California. They showed a scaling relation between τ_p and magnitude M for earthquakes with M of 3.0 to 7.3. In earthquakes with $M < 6$ the total duration of rupture is usually less than 4 s, so the entire rupture time history is included within the first 4 s of the P wave. However, for $M > 6$ earthquakes, the existence of a scaling relation between τ_p and M would imply that the magnitude of an earthquake has been defined before the rupture terminates, and that the rupture process is deterministic. Allen and Kanamori¹⁶ used earthquakes from southern California where data for only three earthquakes with $M_w > 6$ are available.

Here we measure τ_p for a much larger number of earthquakes, including events from Japan, Taiwan, California and Alaska. The waveform data have been provided by K-net (operated by the National Research Institute for Earth Science and Disaster Prevention in Japan), by the Taiwan Strong Motion Instrumentation Program of the Central Weather Bureau, by the Southern California Seismic Network (operated by Caltech and the US Geological Survey), and by the University of Alaska Geophysical Institute. A total of 71 earthquakes producing 1,842 waveforms recorded on both broadband velocity sensors and accelerometers within 100 km of the epicentre are used. There are 24 events with $M_w \geq 6.0$, including the M_w 7.6 Chi-Chi earthquake (Taiwan, 1999) with a rupture duration of ~ 30 s, the M_w 7.9 Denali earthquake (Alaska, 2002) with a rupture duration of ~ 70 s, and the M_w 8.3 Tokachi-oki earthquake (Japan, 2003) with a duration of ~ 40 s. A table of events is included in the Supplementary Information.

We calculate τ_p in a recursive fashion from a vertical velocity timeseries to generate τ_p as a function of time, $\tau_p(t)$ (see Methods section). Figure 1 shows the vertical velocity waveform recorded during a M 4.6 earthquake in southern California and the τ_p timeseries derived from it. Figure 2 shows a similar example but for the M_w 8.3 Tokachi-oki earthquake. In this case only acceleration records are available, and they have been recursively integrated in a causal fashion to derive the velocity trace from which $\tau_p(t)$ is derived. We define the parameter τ_p^{\max} as the maximum $\tau_p(t)$ data point between 0.05 and 4.0 s (see Methods section) after the P-wave trigger as shown in Figs 1 and 2.

When τ_p^{\max} is plotted against M on a log-linear scale, a scaling relation emerges as shown in Fig. 3a. The τ_p^{\max} observations from waveforms at individual stations can exhibit large variability for a single earthquake, which is probably due to measurement error, station effects and path effects¹⁹. Figure 3a shows the average τ_p^{\max} observation for each earthquake using all available data. The best-fit linear relation to the event averages is:

$$\log \tau_p^{\max} = 0.14M - 0.83 \quad (1)$$

and the average absolute deviation is 0.54 magnitude units. The data set has a high linear correlation coefficient of 0.9. For 90% of the earthquakes in this study, τ_p^{\max} is within two times the average absolute deviation. In determining a single linear relation to the entire data set, we have chosen the simplest possible model. Given the hint of a break in our data around M 5.7, we also determined best-fit relations for $M > 5.7$ and $M < 5.7$ events. In both cases the slopes are positive, but lower than equation (1), and the correlation coefficients are reduced, particularly for $M > 5.7$. Although there is variability in τ_p^{\max} observations, equivalent to ± 1 magnitude unit, a scaling relation is clear: this implies that information about the final magnitude of an earthquake is available within the first few seconds of its initiation, irrespective of the total rupture duration.

A second parameter, τ_d , is also measured from the τ_p timeseries. τ_d is the delay of the τ_p^{\max} observation with respect to the P-wave trigger, and is therefore in the range of 0.05 s to 4 s (see Figs 1 and 2).

¹Department of Geology and Geophysics, University of Wisconsin Madison, 1215 W. Dayton Street, Madison, Wisconsin 53706, USA. ²Department of Earth and Planetary Science, University of California Berkeley, 307 McCone Hall, Berkeley, California 94720, USA.

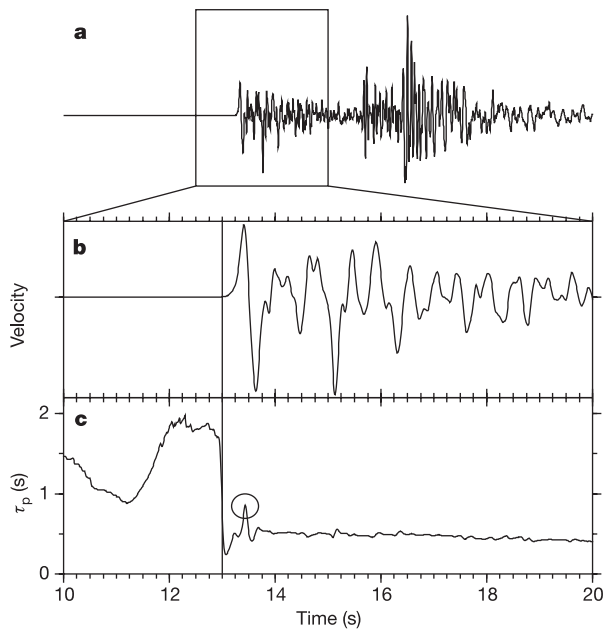


Figure 1 | Example waveform and τ_p^{\max} calculation for a M 4.6 earthquake in southern California recorded at station GSC, 74 km from the epicentre.

a, The raw vertical component waveform recorded by a broadband velocity sensor. **b**, Ten seconds of the velocity waveform after low-pass filtering at 3 Hz. The P-wave trigger time is shown by the vertical line at 13.01 s. **c**, $\tau_p(t)$ trace calculated in a recursive fashion from the waveform in **b**, showing the change in the frequency content from the pre-trigger noise to the post-trigger P wave. The τ_p^{\max} observation is circled (equal to 0.86 s in this case); τ_d is the delay of τ_p^{\max} with respect to the trigger (0.43 s in this case).

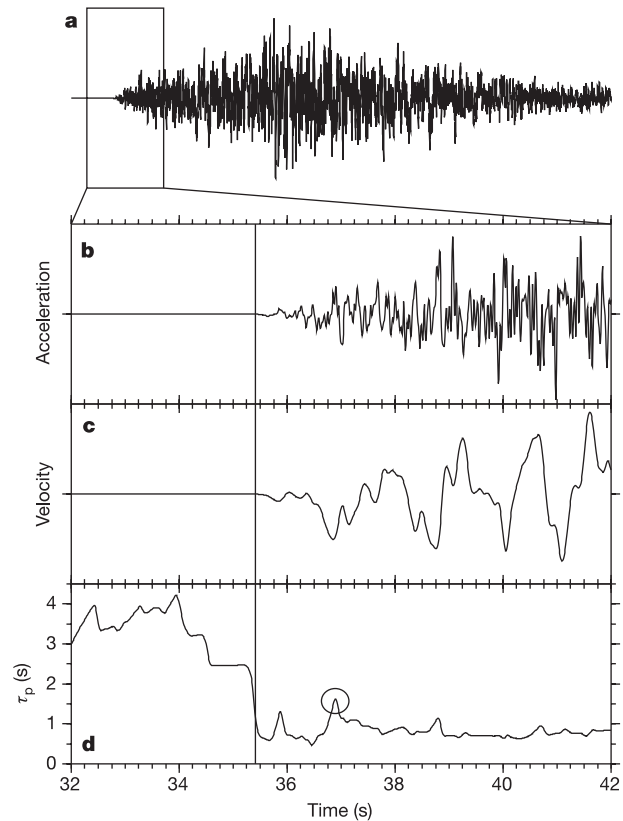


Figure 2 | Example waveform and τ_p^{\max} calculation for the M_w 8.3 Tokachi-oki earthquake, recorded at station HKD112, 71 km from the epicentre. **a**, The raw vertical component waveform recorded on an accelerometer. **b**, Ten seconds of the raw acceleration waveform. The P-wave trigger is shown by the vertical line at 35.41 s. **c**, Ten seconds of the velocity waveform determined from the acceleration recording using recursive relations only. It has also been low-pass filtered at 3 Hz. **d**, $\tau_p(t)$ trace calculated in a recursive fashion from the waveform in **c**. The τ_p^{\max} observation is circled ($\tau_p^{\max} = 1.62$ s, $\tau_d = 1.49$ s), it has a longer period and is observed later than the example in Fig. 1c owing to the larger magnitude of the earthquake.

Figure 3b plots the event-averaged τ_d observations versus magnitude, showing a general increase in τ_d with magnitude. Also indicated on Fig. 3b is the typical rupture duration as a function of magnitude. The relation shown is only approximate, as the rupture duration for a given magnitude event can vary by a factor of 2 or 3 (see Methods section). Despite the uncertainty in the rupture duration of the specific earthquakes included in this study, it is clear that for earthquakes with $M > 4$ the τ_p^{\max} observation is made before the rupture has ceased. While up to 4 s of data are used to determine τ_p^{\max} , the average time window of the P wave required to determine τ_p^{\max} is less than 2 s for almost all earthquakes in our study.

Using published moment rate functions for the $M > 6$ events in our study, we can estimate the amount of moment release at time τ_d . Rupture directivity effects of finite faults mean that the first 2 s of the P wave at a given station does not sample exactly 2 s of the rupture. However, because our τ_d measurement is event-averaged we can use it as an approximate estimate of the rupture duration within which τ_p^{\max} information is available. Calculating the seismic moment released within τ_d shows an increase with magnitude, which is not surprising given that τ_d also increases with magnitude. But the percentage of moment released is always small (less than 40% for $M > 6$ events) and decreases with magnitude. In the case of the largest earthquakes—Chi-Chi, Tokachi-oki and Denali—the percentage of moment released is less than 2%. The fraction of the total rupture duration at which point τ_p^{\max} information is available is not constant, and decreases with increasing magnitude.

Although there is a ± 1 magnitude unit scatter in the τ_p^{\max} data, the observations show that the rupture process is at least partly deterministic: that is, the final magnitude of an event is to some degree controlled by processes within the first few seconds (typically < 2 s) of rupture. The scatter could be due to source processes and/or local site and measurement errors. If the scatter is non-source related, then removal or correction for site and path effects could reduce the

scatter in the data points of Fig. 3a to a single line, implying that the final magnitude of an earthquake is entirely determined within the first few seconds of rupture. Variability in the quality of the τ_p^{\max} observations at different stations has already been observed across the seismic network in southern California, indicating that site effects do play a role¹⁹. Nevertheless, it seems unlikely that all the scatter is due only to site effects. Instead, source-related processes (including rupture behaviour, stress heterogeneity and other on-fault variability) probably also play a role.

The cascade model of sequential slip on adjacent fault patches must be refined in order to be consistent with our observations. In particular, a cascade in which a small or large earthquake could initiate as slip on any small patch and grow according to the conditions on the surrounding fault plane until rupture arrest is inconsistent with our observed scaling relation. This does not preclude the existence of multiple slip patches within a rupture. For some earthquakes, a sequence of ‘subevents’ (which could be considered as slip on specific patches) has been observed within the τ_d time window and τ_p^{\max} is a measure of the final subevent—for example, the Landers earthquake²⁰. In other cases, however, τ_p^{\max} is observed before completion of the first subevent, and before the later, larger subevents are under way—as in the case of the Denali earthquake²¹. Therefore, although rupture may still be considered as slip on a series of fault patches, the final seismic moment is at least partially determined by the patch or patches that rupture within the first few seconds.

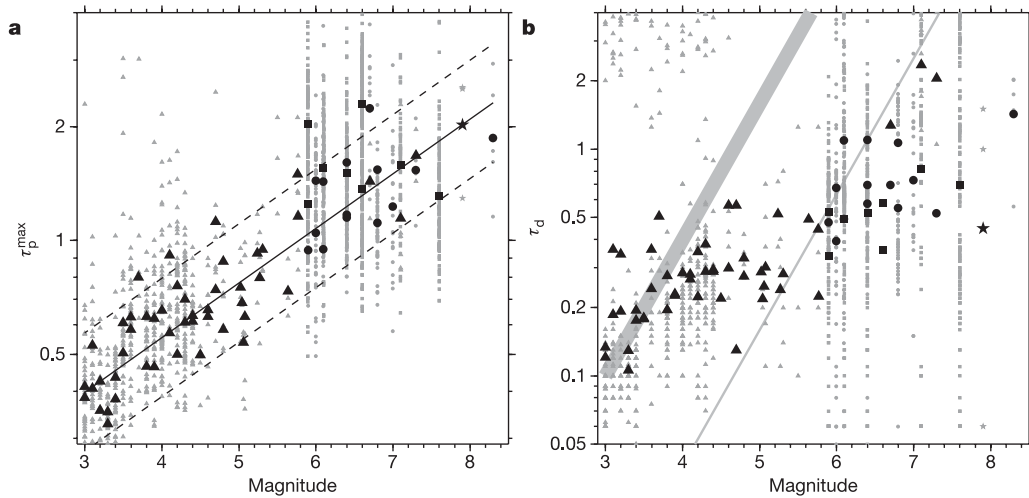


Figure 3 | The relation between τ_p^{\max} , τ_d and magnitude. **a**, The scaling relation between τ_p^{\max} and magnitude for earthquakes in southern California (triangles), Japan (circles), Taiwan (squares) and Alaska (stars). Observations at individual stations can show a large scatter for a given event (small grey shapes). The event averaged values are also shown (large black shapes). The best-fit to event averages is shown as a solid line. The average absolute deviation of the observations is 0.54 magnitude units; plus and minus two times the average absolute deviation is shown as dashed lines.

b, τ_d plotted against magnitude, showing the general increase in the time required to make the τ_p^{\max} observation with increasing magnitude. The symbols are the same as in **a**. Grey shapes indicate individual station observations, black is the event average. The thick grey bar shows the approximate rupture duration as a function of magnitude, indicating that the τ_p^{\max} observation is made before rupture ceases for all $M > 4$ earthquakes in this study. The thin grey line indicates one-tenth of the rupture duration, and is crossed by the trend of the τ_d data.

We propose that the final magnitude of an earthquake is partially controlled by the initiation process within the first few seconds of rupture, and partially by the physical state of the surrounding fault plane. The role played by the initiation process can be understood by considering the energy balance of fault rupture. A rupture can only propagate when the available energy is sufficient to supply the necessary fracture energy^{22,23}. When a propagating fracture encounters a patch with a lower stress-drop, the total energy in the system will begin to decrease. Depending on the size of the patch, it may cause the rupture to terminate. The total rupture energy available increases with the amount of slip, so a large-slip rupture will propagate further across a heterogeneous fault plane. Therefore, if the rupture pulse initiates with large slip, it is more likely to evolve into a large earthquake. This explanation is consistent with the observation that large earthquakes do not nucleate at shallow depths, but instead at greater depths where the frictional strength and stress drop are greater²⁴. A recent study²⁵ also shows that hypocentres are preferentially located within or close to regions of large slip.

The τ_p^{\max} scaling relation provides new constraints on the physics of the rupture process. Whereas the cascade model suggests that the magnitude of an earthquake is dependent on the state of stress across the fault plane and that the nucleation of all earthquakes is identical, our present observations demonstrate the significance of the rupture initiation process within the first few seconds of an event. Understanding the physics of this process will enable us to predict the magnitude of earthquakes without accurate knowledge of the surrounding state of stress across a fault plane.

METHODS

Waveform processing. The τ_p^{\max} observations are derived from the vertical component of either broadband velocity seismometers or accelerometers. The acceleration waveforms are converted to velocity, and all data are low-passed at 3 Hz using the recursive relations described in ref. 26. The $\tau_p(t)$ timeseries is then calculated from the low-passed velocity waveform using the following recursive relation:

$$\tau_i^p = 2\pi \sqrt{X_i/D_i}$$

Here $X_i = \alpha X_{i-1} + x_i^2$, $D_i = \alpha D_{i-1} + (dx/dt)_i^2$, x_i is the ground motion recorded at time i and α is a 1 s smoothing constant. For 100 sample per second (s.p.s.) data $\alpha = 0.99$, for 20 s.p.s. data $\alpha = 0.95$. This approach was first described in ref. 15; more information is available in ref. 16.

We define the parameter τ_p^{\max} as the maximum $\tau_p(t)$ data point between 0.05 s and 4.0 s after the P-wave trigger, as shown in Figs 1 and 2. The time window starts at 0.05 s rather than 0.00 s owing to the recursive nature of the $\tau_p(t)$ calculation. Using the maximum value between 0.0 s and 4.0 s can result in leakage of the frequency content of background noise before the P-wave arrival into the time window after the P wave. We also experimented with time windows ranging in duration from 1 s to 5 s. The upper limit was set to 5 s, as the S-wave arrival, which contaminates the P-wave signal, is 5 s behind the P wave at an epicentral distance of ~ 50 km, half the epicentral distance range of the data. Experimenting with these different time windows, we found that there was no improvement in the relation between τ_p^{\max} and magnitude when 5 s of data were used rather than 4 s. There was, however, improvement in the relation when 4 s was used rather than a shorter time window.

Estimation of rupture duration. The relation between rupture duration and magnitude shown in Fig. 3b is based on scaling relations between rupture length and magnitude. The rupture length is converted to rupture duration by assuming unilateral rupture and a rupture velocity between 2.4 km s^{-1} and 3.0 km s^{-1} from the estimates of ref. 27. Two approaches to estimating rupture length are applied. First, the empirical scaling relations between magnitude and rupture length developed in ref. 28 are used. These are appropriate for $M > 4.5$ earthquakes. Second, we use the scaling relations between rupture dimension and seismic moment for stress drops in the range 0.1–10 MPa. The rupture durations shown in Fig. 3b are an average of the range of rupture durations obtained using the approaches described above. The actual rupture duration for a given magnitude event can vary by a factor of 2 or 3.

Received 12 April; accepted 30 August 2005.

1. Brune, J. N. Implications of earthquake triggering and rupture propagation for earthquake prediction based on premonitory phenomena. *J. Geophys. Res.* **84**, 2195–2198 (1979).
2. Fukao, Y. & Furumoto, M. Hierarchy in earthquake size distribution. *Phys. Earth Planet. Inter.* **37**, 149–168 (1985).
3. Ellsworth, W. L. & Beroza, G. C. Seismic evidence for an earthquake nucleation phase. *Science* **268**, 851–855 (1995).
4. Beroza, G. C. & Ellsworth, W. L. Properties of the seismic nucleation phase. *Tectonophysics* **261**, 209–227 (1996).
5. Dodge, D. A., Beroza, G. C. & Ellsworth, W. L. Detailed observations of California foreshock sequences: Implications for the earthquake initiation process. *J. Geophys. Res.* **101**, 22371–22392 (1996).
6. Mori, J. Rupture directivity and slip distribution of the M 4.3 foreshock to the 1992 Joshua Tree earthquake, Southern California. *Bull. Seismol. Soc. Am.* **86**, 805–810 (1996).
7. Mori, J. & Kanamori, H. Initial rupture of earthquakes in the 1995 Ridgecrest, California sequence. *Geophys. Res. Lett.* **23**, 2437–2440 (1996).
8. Singh, S. K. *et al.* Implications of a composite source model and seismic-wave

- attenuation for the observed simplicity of small earthquakes and reported duration of earthquake initiation phase. *Bull. Seismol. Soc. Am.* **88**, 1171–1181 (1998).
9. Steacy, S. J. & McCloskey, J. What controls an earthquake's size? Results from a heterogeneous cellular automaton. *Geophys. J. Int.* **133**, F11–F14 (1998).
 10. Kilb, D. & Gomberg, J. The initial subevent of the 1994 Northridge, California, earthquake: Is earthquake size predictable? *J. Seismol.* **3**, 409–420 (1999).
 11. Sato, T. & Kanamori, H. Beginning of earthquakes modeled with the Griffith's fracture criterion. *Bull. Seismol. Soc. Am.* **89**, 80–93 (1999).
 12. Ohnaka, M. A physical scaling relation between the size of an earthquake and its nucleation zone size. *Pure Appl. Geophys.* **157**, 2259–2282 (2000).
 13. Ellsworth, W. L. & Beroza, G. C. Observation of the seismic nucleation phase in the Ridgecrest, California, earthquake sequence. *Geophys. Res. Lett.* **25**, 401–404 (1998).
 14. Kanamori, H. The energy release in great earthquakes. *J. Geophys. Res.* **82**, 2981–2987 (1977).
 15. Nakamura, Y. in *Proc. 9th World Conf. Earthquake Eng.* VII, 673–678 (1988).
 16. Allen, R. M. & Kanamori, H. The potential for earthquake early warning in southern California. *Science* **300**, 786–789 (2003).
 17. Kanamori, H. The diversity of the physics of earthquakes. *Proc. Jpn. Acad. B* **80**, 297–316 (2004).
 18. Nakamura, Y. in *Proc. 13th World Conf. Earthquake Eng.* Paper No. 908 (2004).
 19. Lockman, A. & Allen, R. M. Single station earthquake characterization for early warning. *Bull. Seismol. Soc. Am.* (in the press).
 20. Abercrombie, R. & Mori, J. Local observations of the onset of a large earthquake: 28 June 1992 Landers, California. *Bull. Seismol. Soc. Am.* **84**, 725–734 (1994).
 21. Eberhart-Phillips, D. *et al.* The 2002 Denali Fault Earthquake, Alaska: A large magnitude, slip-partitioned event. *Science* **300**, 1113–1118 (2003).
 22. Nielsen, S. B. & Olsen, K. B. Constraints on stress and friction from dynamic rupture models of the 1994 Northridge, California, earthquake. *Pure Appl. Geophys.* **157**, 2029–2046 (2000).
 23. Oglesby, D. D. & Day, S. M. Stochastic fault stress: Implications for fault dynamics and ground motion. *Bull. Seismol. Soc. Am.* **92**, 3006–3021 (2002).
 24. Das, S. & Scholz, C. H. Why large earthquakes do not nucleate at shallow depths. *Nature* **305**, 621–623 (1983).
 25. Mai, P. M., Spudich, P. & Boatwright, J. Hypocenter locations in finite-source rupture models. *Bull. Seismol. Soc. Am.* **95**, 965–980 (2005).
 26. Kanamori, H., Maechling, P. & Hauksson, E. Continuous monitoring of ground-motion parameters. *Bull. Seismol. Soc. Am.* **89**, 311–316 (1999).
 27. Somerville, P., Irikura, K., Graves, R. P., Sawada, S. & Wald, D. Characterizing crustal earthquake slip models for the prediction of strong motion. *Seismol. Res. Lett.* **70**, 59–80 (1999).
 28. Wells, D. L. & Coppersmith, K. J. New empirical relationships among magnitude, rupture length, rupture width, rupture area, and surface displacement. *Bull. Seismol. Soc. Am.* **84**, 974–1002 (1994).
- Supplementary Information** is linked to the online version of the paper at www.nature.com/nature.
- Acknowledgements** We thank H. Kanamori and S. Nielsen for discussions, and Y.-M. Wu and R. Hansen for making waveform data available for the study. The manuscript was improved by comments from R. Abercrombie and C. Scholz. Funding for this work was provided by the US Geological Survey NEHRP programme, the University of Wisconsin, Madison, and the University of California, Berkeley.
- Author Information** Reprints and permissions information is available at npg.nature.com/reprintsandpermissions. The authors declare no competing financial interests. Correspondence and requests for materials should be addressed to R.M.A. (rallen@berkeley.edu).